

Length Scale Dependence of the Dynamic Properties of Hyaluronic Acid Solutions in the Presence of Salt

Ferenc Horkay,[†] Peter Falus,[‡] Anne-Marie Hecht,[§] and Erik Geissler^{*,§}

Section on Tissue Biophysics and Biomimetics, Program in Pediatric Imaging and Tissue Sciences, Eunice Kennedy Shriver National Institute of Child Health and Human Development, National Institutes of Health, 13 South Drive, Bethesda, Maryland 20892, United States, Institut Laue-Langevin, BP 156, 6 rue Jules Horowitz, 38042 Grenoble Cedex 9, France, and Laboratoire de Spectrométrie Physique CNRS UMR 5588, Université J. Fourier de Grenoble, B.P.87, 38402 St. Martin d'Hères Cedex, France

Received: July 15, 2010; Revised Manuscript Received: October 20, 2010

In solutions of the charged semirigid biopolymer hyaluronic acid in salt-free conditions, the diffusion coefficient D_{NSE} measured at high transfer momentum q by neutron spin echo is more than an order of magnitude smaller than that determined by dynamic light scattering, D_{DLS} . This behavior contrasts with neutral polymer solutions. With increasing salt content, D_{DLS} approaches D_{NSE} , which is independent of ionic strength. Contrary to theoretical expectation, the ion–polymer coupling, which dominates the low q dynamics of polyelectrolyte solutions, already breaks down at distance scales greater than the Debye–Hückel length.

Introduction

Ion–polyelectrolyte interactions play a decisive role in many systems, from living organisms to materials science. Owing to their structural complexity, their multicomponent nature, and the simultaneous presence of short- and long-range interactions, polyelectrolyte solutions remain incompletely understood.^{1–3} Long-range electrostatic interactions dominate the conformational and thermodynamic properties, and local ordering processes such as helix formation are governed by the mobility at the segmental level. Transport properties in heterogeneous media (e.g., tissues or cells) depend both on long-range and on short-range interactions.

In semidilute polymer solutions, the diffusive properties of the chains are a function of the characteristic mesh size of the solution and of the thermodynamic interactions between the polymer and the solvent.¹ These properties can be investigated by dynamic light scattering (DLS), which measures the collective diffusion coefficient, D_{DLS} , on a length scale range much greater than the mesh size, ξ (low transfer momentum q). Neutron spin echo (NSE) probes the polymer dynamics in a higher q range.⁴ With neutral polymers, no difference is detected between D_{DLS} and that measured by NSE, D_{NSE} .^{5,6} In polyelectrolyte solutions, however, where the dynamics of the polymer is coupled to that of the ion cloud, this correspondence remains to be verified experimentally.⁷

In principle, measurements of the dynamics of polymers by DLS and NSE are equivalent, albeit for different length scale ranges $1/q$. With both techniques, the scattering intensity is determined by the contrast between the polymer and the solvent. For DLS, this contrast is defined exclusively by the chemical nature of both components, a parameter that can be modified only by changing the system. Neutron scattering experiments, on the other hand, by replacing hydrogen with deuterium in the appropriate components, can select the signal either of the

counterions or of the mutual (collective) diffusion of the polymer in the solution. In this way, measurements have been made by NSE of the dynamics of hydrogenated counterions in solutions of deuterated polystyrene sulfonate in salt-free conditions. These measurements revealed a strong q -dependence of the diffusion coefficient of the counterions.⁸

This paper describes DLS and NSE investigations of the mutual diffusion between hydrogenated polyelectrolyte chains and a deuterated solvent. The measurements were conducted in the semidilute polymer concentration regime under various conditions of added salt to distinguish the long-range repulsive electrostatic interactions from the short-range excluded volume effects in the collective diffusion.

To describe the scattering properties of polyelectrolyte solutions, we invoke the analogy of suspensions of charged spheres, the scattering intensity of which can be expressed in terms of the product of the form factor $P(q)$ of a sphere and the structure factor $S(q)$ describing the interparticle correlations. Thus,

$$I(q) = P(q) \cdot S(q) \quad (1)$$

According to scaling theory, polymer chains in solution in the semidilute regime are pictured as a sequence of correlation volumes (thermal blobs), analogous to the form factor of the suspension of spheres.¹ For charged polymers, however, changes in the ionic strength or ion valence modify both the interchain and intrachain potential, and consequently, the size of the blobs is variable. For small q , therefore, where the spatial range $1/q$ of the measurement spans many chains, the distinction between $P(q)$ and $S(q)$ is purely formal, and the important physical property is the scattered intensity itself. For the polyelectrolyte solutions investigated here, eq 1 nevertheless provides a framework to interpret the q dependence of $I(q)$. Although theoretical treatments have been proposed,^{7,9,10} detailed experimental investigations of the effects of salt on the dynamic properties of polyelectrolytes by both DLS and NSE are lacking in the literature.

* Corresponding authors. E-mails: (E.G.) erik.geissler@ujf-grenoble.fr, (F.H.) horkay@helix.nih.gov.

[†] National Institutes of Health.

[‡] Institut Laue-Langevin.

[§] Université J. Fourier de Grenoble.

The present DLS and NSE measurements were made on solutions of a semirigid biological polyelectrolyte. The local configuration of this class of polymer is simpler than that of flexible polyelectrolytes, in which the effective chain cross section (electrostatic blob radius) depends on salt conditions.¹¹ The system investigated was the sodium salt of hyaluronic acid (HA), one of the most abundant biopolymers in the human body. HA participates in the organization and self-assembly of proteoglycans in cartilage and is involved in cellular processes such as cell proliferation, morphogenesis, inflammation, and wound repair as well as interacting with cell surface receptors. The biological function of HA includes control of transport properties (e.g., water and ion diffusion, tissue hydration) and rheological behavior (e.g., viscosity of the synovial fluid and vitreous humor in the eye). These processes take place in the presence of both mono- and divalent ions. The diversity of biological functions of HA implies a variety of interactions, which are sensitive to local environmental conditions such as the ionic strength of the solution. Unlike polyelectrolytes with hydrophobic backbones, HA remains soluble even at high ionic strength in the presence of divalent counterions.^{12,13}

Experimental Section

Solutions of hyaluronic acid (sodium salt) (Sigma, $M_w = 1.2 \times 10^6$) at concentration $c = 2\%$ w/w were prepared with D_2O (99.9% D) as the solvent in all samples. This concentration lies in the semidilute regime, where the polymer chains strongly overlap. The concentration of NaCl was varied in and beyond the physiological range, from 0 to 0.4 M. Solutions were also prepared with $CaCl_2$, at 0 and 0.2 M, together with 0.1 M NaCl. The Debye–Hückel screening length, Λ , for these salt concentrations ranges from 2.5 to 15 Å.

DLS measurements were made with an ALV goniometer (ALV, Langen, Germany) working at incident wavelength $\lambda = 6328$ Å. The NSE observations were made at the IN15 instrument at the Institut Laue Langevin, Grenoble, with $\lambda = 11$ and 15 Å. The length scales explored in the scattering measurements cover the ranges $1000 \text{ Å} \geq 1/q \geq 400 \text{ Å}$ (DLS) and $30 \text{ Å} \geq 1/q \geq 9 \text{ Å}$ (NSE), where $q = (4\pi n/\lambda) \sin(\theta/2)$ is the momentum transfer (n being the refractive index of the solvent, and θ , the scattering angle). SAXS measurements were made at the insertion device of Sector 5 at the Advanced Photon Source (DND-CAT), with $\lambda = 1.55$ Å, in the range $0.0016 \leq q \leq 0.35 \text{ Å}^{-1}$. Complementary estimates of the osmotic modulus were made from measurements of the osmotic pressure Π .¹³

Results and Discussion

The characteristic length scale in polymer solutions can be determined from the intensity correlation function of the light scattered by the concentration fluctuations, as measured by DLS. In the scaling picture of semidilute polymer solutions,¹ at small q , the relaxation rate, Γ , of concentration fluctuations obeys Fick's equation of diffusion and varies as q^2 ; thus,

$$\Gamma = D_{\text{DLS}}q^2 \quad (2)$$

where D_{DLS} is the collective diffusion coefficient. The hydrodynamic correlation length is then defined by the Stokes–Einstein relationship,

$$\xi = k_B T / (6\pi\eta D_{\text{DLS}}) \quad (3)$$

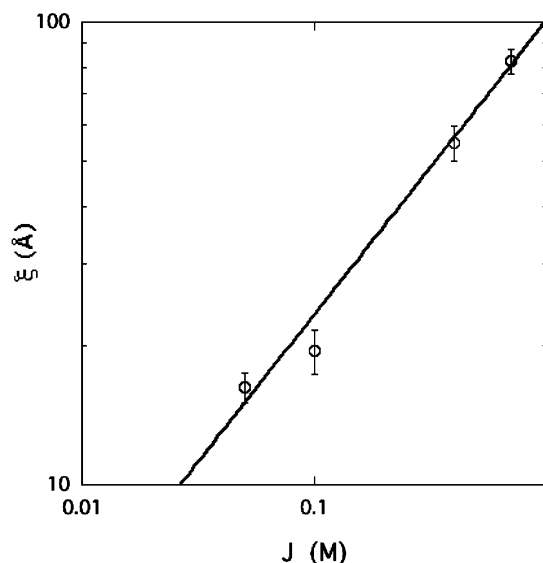


Figure 1. Variation of the hydrodynamic correlation length $\xi = k_B T / (6\pi\eta D)$ with ionic strength J in 2% w/w solutions of HA. The slope of the power law fit is 0.64 ± 0.04 .

where $k_B T$ and η are the Boltzmann factor and the solvent viscosity, respectively. In semidilute polyelectrolyte solutions, ξ depends not only on the polymer concentration, but also on the ionic strength, $J (= 1/2 \sum_i Z_i^2 c_i)$, where Z_i and c_i are the charge and molar concentration, respectively, of the ionic species i of added salt.^{7,12} For solutions of HA at fixed concentration (2% w/w), ξ exhibits a power law dependence on J (Figure 1). Over the range of values of ξ displayed in this figure, the Rayleigh condition ($q\xi \ll 1$) holds for DLS measurements, and consequently, $I(q)$ is independent of q . Measurements of the dynamic light scattering intensity confirm this invariance.

At higher values of q , such that $q\xi > 1$, scattering experiments detect internal modes inside the correlation volume, which possess no unique length scale. The only characteristic length scale is that defined by the conditions of detection; namely, $1/q$. Hence,

$$\Gamma = k_B T q^3 / (6\pi\eta) \quad (4)$$

The transition between the simple diffusive response of eq 2 and the universal behavior of eq 4 is commonly observed in solutions of neutral flexible polymers.^{5,6}

At even higher values of q , the individual segments of the polymer chain become resolved, and diffusive motion of the segments prevails. In this regime,

$$\Gamma = k_B T q^2 / (6\pi\eta a) \quad (5)$$

where a is the hydrodynamic radius of the polymer segment. In the case of HA, where the persistence length of the polymer chain is on the order of 50 Å,¹⁴ it is to be expected that eq 5 applies over the whole q range of the NSE measurements. In other words, for the observations reported here,

$$D_{\text{NSE}} = k_B T / (6\pi\eta a) \quad (6)$$

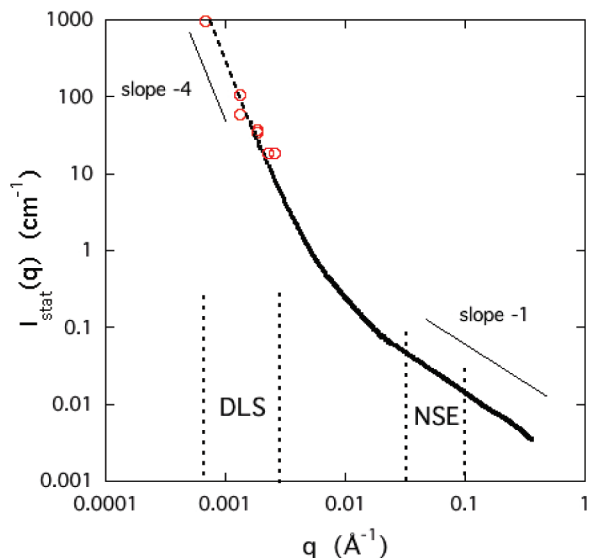


Figure 2. SAXS spectrum of a 2% w/w HA solution in 0.1 M NaCl (solid symbols). SLS response of the same solution (open symbols). The size of each symbol reflects the range of the experimental error.

The close similarity in value of ξ and a in the semidilute concentration range make it unlikely that the universal regime of eq 4 can be detected in the present measurements.

The effect of salt on the diffusion properties of polyelectrolyte solutions can be expressed in terms of mode coupling between the polyion and its surrounding cloud of small mobile ions.^{7,10} When hydrodynamic interactions are neglected, the dependence of the diffusion coefficient on salt concentration is found from the coupled equations

$$\partial \bar{c}_i(q, t) / \partial t = -D_i \sum_k [q^2 \delta_{ik} + (c_i/c_k)^{1/2} \kappa_i \kappa_k] \bar{c}_i(q, t) \quad (7)$$

where D_1 , D_2 , and D_3 are the diffusion coefficients of the (negative) macroion, the (positive) counterions, and the (negative) co-ions, respectively. In eq 7, $\kappa_i = Z_i(l_B c_i)^{1/2}$ is the inverse Debye–Hückel screening length associated with the ionic species i , of charge Z_i , and average concentration c_i . \bar{c}_i is the spatial Fourier transform of the concentration fluctuations, and l_B is the Bjerrum length.¹⁵ According to eq 7, at small q , the effective diffusion coefficient of the macroion, Γ/q^2 , gradually increases from its limiting value D_1 at high added salt concentration to a much larger value, intermediate between D_1 and the diffusion coefficient of the small ions, in zero added salt.⁷ At very high q ($\gg \kappa_i$), by contrast, the off-diagonal terms in eq 7 are negligible, with the result that the motion of the polymer is decoupled from that of the small ions. Γ/q^2 therefore asymptotically approaches D_1 . DLS measurements on solutions of sodium polystyrene sulfonate (NaPSS), which is a flexible polymer with a hydrophobic vinyl backbone, indicate that the asymptotic minimum of Γ/q^2 is attained at ~ 1 M NaCl.¹⁶ At this salt concentration, $1/\kappa$ (≈ 3.1 Å) is comparable to the length of the NaPSS monomer. These DLS observations, in which the measurement length scale $1/q$ greatly exceeds the Debye–Hückel length $1/\kappa$, indicate that at high salt concentrations the polyelectrolyte behaves like a neutral polymer.

Figure 2 shows the combined static light scattering (SLS) and SAXS response from a 2% HA solution in 100 mM NaCl, illustrating the q range explored in the DLS and NSE experi-

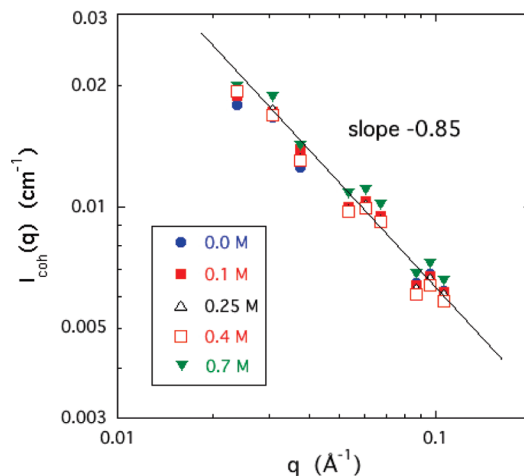


Figure 3. Dependence on q of the NSE scattering intensity from 2% w/w HA solutions, measured at different ionic strengths, J .

ments. At low q ($\leq 3 \times 10^{-3}$ Å⁻¹), the integrated (i.e., static) scattering intensity $I_{\text{stat}}(q)$ decreases approximately as q^{-4} , characteristic of large clusters with smooth interfaces.¹⁷ Such clustering is a general feature of semidilute polyelectrolyte solutions. At high q ($\geq 2 \times 10^{-2}$ Å⁻¹), $I_{\text{stat}}(q)$ varies as q^{-1} , reflecting the rod-like character of the overlapping HA chains at short length scales. The variation of the neutron coherent scattering intensity, measured by NSE at different salt concentrations, is displayed in Figure 3. Although the signal-to-noise ratio in these measurements is much poorer than that of the SAXS spectra, the slope of the power law fit to the data, -0.85 , is within experimental error consistent with the rod-like character of the HA chain. It is also apparent from this figure that the neutron scattering intensity is independent of ionic strength.

Figure 4a shows a typical DLS normalized intensity correlation function $g_2(t)$ of the scattered light, obtained from an HA solution containing 0.1 M NaCl + 0.05 M CaCl₂. Two distinct relaxation processes are visible, separated by ~ 3 orders of magnitude in time. The fast relaxation rate, Γ , is the collective mode defining the osmotic concentration fluctuations; the slow relaxation rate, Γ_s , reflects the internal motion of the large clusters, the surfaces of which are responsible for the q^{-4} scattering in Figure 2. The continuous curve in Figure 4a is the fit to the Siegert relationship for a polymer solution with two relaxation modes,¹²

$$g_2(t) - 1 = \beta |g_1(t)|^2 \quad (8a)$$

where

$$g_1(t) = b \exp(-\Gamma t) + (1 - b) \exp[-(\Gamma_s t)^{2/3}] \quad (8b)$$

In eq 8, $\beta \approx 0.96$ is the optical coherence factor of the detection system; $g_1(t)$ is the field correlation function, with the usual condition that $g_1(0) = 1$; b is the relative amplitude of the thermodynamic fluctuations; and the exponent $2/3$ of the stretched exponential is typical of internal modes.¹ The dashed curve in Figure 4 corresponds to the second term in eq 8b. Figure 4b shows the field correlation function obtained from the salt-free sample at scattering angle $\theta = 120^\circ$.

The dependence of the fast relaxation rate Γ on q of the thermodynamic concentration fluctuations, measured by DLS, is plotted in Figure 5. The proportionality of Γ to q^2 implies

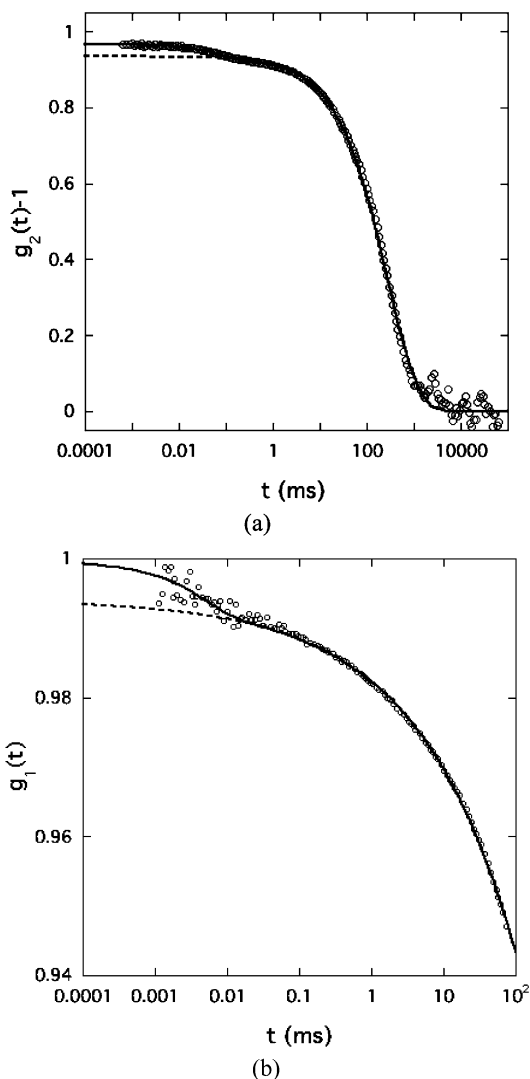


Figure 4. (a) Intensity correlation function, $g_2(t) - 1$, from HA solution containing 0.1 M NaCl + 0.05 M CaCl₂, measured at $\theta = 90^\circ$. Continuous line: fit to eq 8. Dashed line: slow component of eq 8. (b) Field correlation function, $g_1(t)$, from eq 8b for HA sample containing zero added salt ($J = 0$), measured at $\theta = 120^\circ$, displaying the total fit and the slow component.

that this motion is diffusive, where the diffusion coefficient $D_{\text{DLS}} = \Gamma/q^2$ increases with decreasing ionic strength, J .^{7,12} The slow relaxation rate, Γ_s , is proportional to q^3 (Figure 6) and increases with increasing salt content. The intensity of the slow feature greatly exceeds that of the fast mode, and as indicated in Figure 2, it continues to increase strongly at low q . Its contribution to the osmotic pressure is therefore negligible. The study of its mechanism, however, lies outside the scope of this paper.

Figure 7a shows a typical spin echo decay, obtained from the same sample as the DLS correlation function in Figure 4a, that is, a 2% HA solution containing 0.1 M NaCl + 0.05 M CaCl₂. Within experimental error, the echoes exhibit simple exponential decays. At $q = 0.087 \text{ \AA}^{-1}$, the decay time is ~ 30 ns. Equivalent decays for the sample with $J = 0$ are shown in Figure 7b for different values of q . The dependence of the NSE relaxation rate Γ on q^2 is plotted in Figure 8 for three different salt concentrations. In contrast to the DLS results, the slope of the straight lines varies weakly with J , displaying no systematic trend. Its value is smaller than that found by DLS.

The results are summarized in Figure 9, where D_{NSE} and D_{DLS} are plotted as a function of ionic strength. D_{DLS} is a decreasing

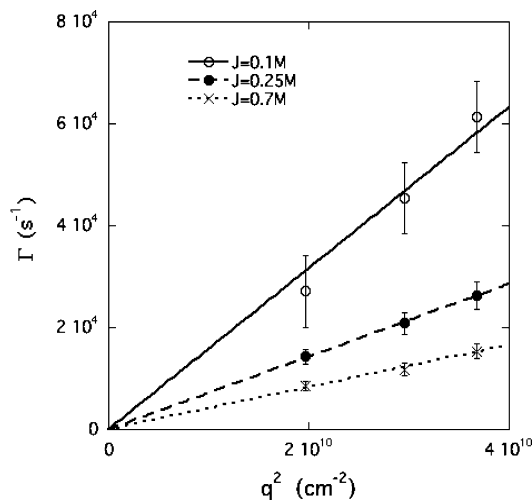


Figure 5. DLS relaxation rate Γ vs q^2 of fast decay for 2% w/w HA solutions in 0.1 M NaCl, 0.1 M NaCl + 0.05 M CaCl₂, and 0.1 M NaCl + 0.2 M CaCl₂.

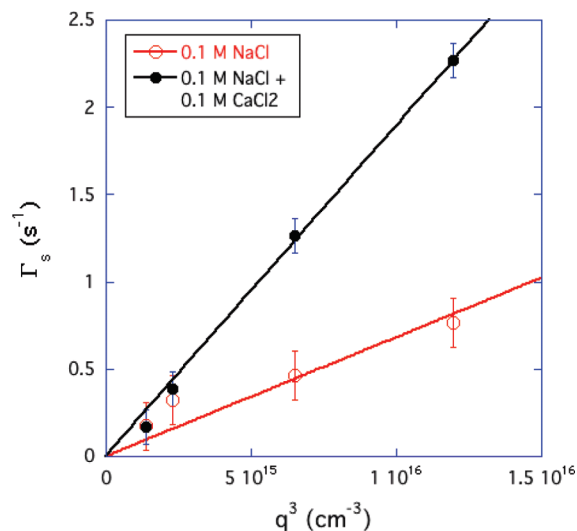


Figure 6. Dependence on q^3 of the slow relaxation rate Γ_s for 2% w/w HA solutions in 0.1 M NaCl (open symbols) and in 0.1 M NaCl + 0.1 M CaCl₂ (solid symbols).

function of J , tending to a constant value at high J . This behavior is reflected in the mode-coupling formalism of eq 7, on taking for the asymptotic value of the diffusion coefficient of the macroion $D_1 = 3 \times 10^{-7} \text{ cm}^2 \text{ s}^{-1}$ (continuous line through DLS data).

The observed variation of the diffusion coefficient at low q can be interpreted in terms of the intensity scattered by the dynamic osmotic fluctuations (as opposed to the total scattered intensity)

$$I_{\text{DLS}}(q \rightarrow 0) = Kk_B T \frac{c^2}{c \partial \Pi / \partial c} \quad (9)$$

where $c \partial \Pi / \partial c$ is the osmotic modulus of the solution and K is the optical contrast factor between the polymer and solvent. Experimentally, I_{DLS} is independent of q . Since the collective diffusion coefficient, D_{DLS} , is proportional¹ to $\partial \Pi / \partial c$ and the polymer concentration, c , is constant in these measurements, eq 9 implies that the osmotic modulus should display a dependence on J having the same functional form as D_{DLS} ; that is,

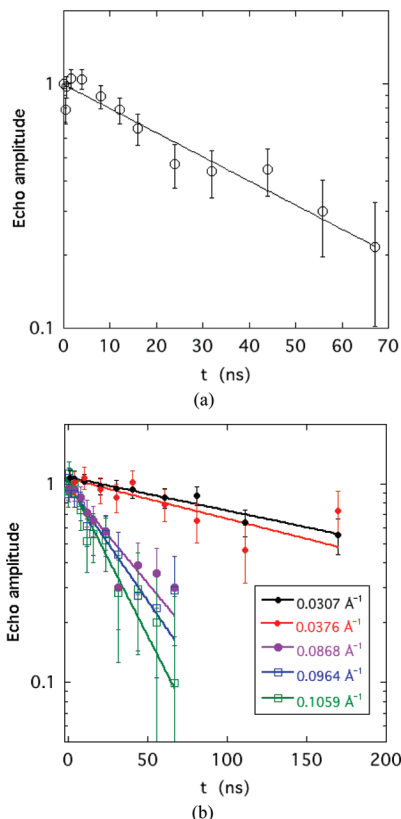


Figure 7. (a) NSE decay at $q = 0.087 \text{ \AA}^{-1}$ for the same sample as in Figure 4a; (b) NSE decays for the same sample as in Figure 4b ($J = 0$) at different q .

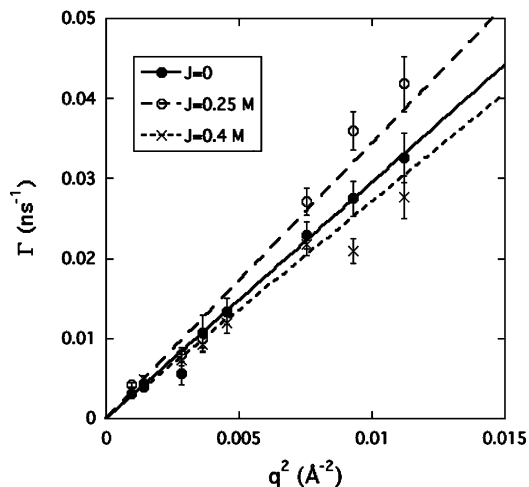


Figure 8. NSE relaxation rate Γ vs q^2 for 2% HA solutions in zero added salt (\bullet), 0.1 M NaCl + 0.05 M CaCl₂ (\circ), and 0.1 M NaCl + 0.1 M CaCl₂ (\times).

$$D_{\text{DLS}}(q, J) \propto (c\partial\Pi/\partial c) \quad (10)$$

This relationship may be verified independently by measuring the osmotic pressure, $\Pi(c)$. The resulting variation of $c\partial\Pi/\partial c$, also displayed in Figure 9, indeed shows a dependence on J similar to that of D_{DLS} . The mode coupling relation 7 thus provides a reasonable description of the low q behavior.

The situation at high q is strikingly different. Figure 9 shows that D_{NSE} is independent of q , while, according to Figure 3, the scattering intensity decreases approximately as $1/q$. Unlike in the low- q regime, therefore, the product $I(q, J) \times D(q, J)$ is now a function of q . In this high- q range, the individual chain segments are resolved, and the intensity is proportional to the

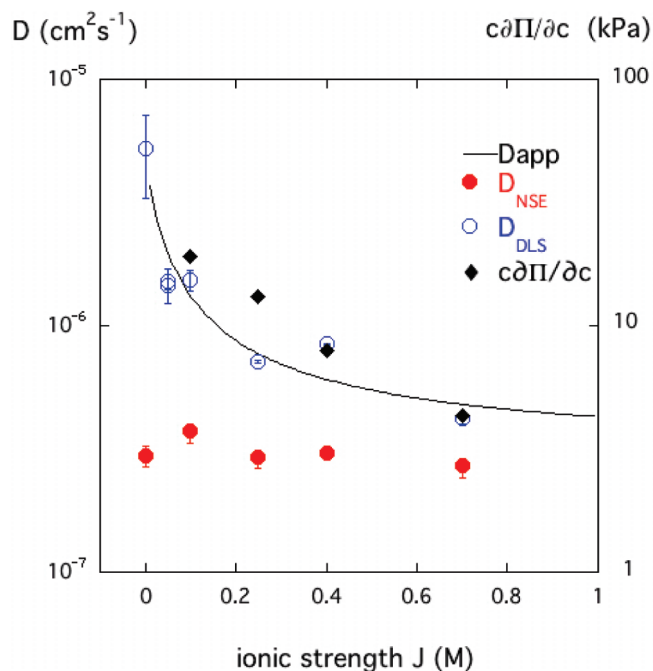


Figure 9. (Left axis) Dependence of diffusion coefficient D on J in 2% w/w HA solutions. \circ : D_{DLS} . \bullet : D_{NSE} . Continuous line: mode coupling model (eq 7) with $D_1 = 3 \times 10^{-7} \text{ cm}^2 \text{ s}^{-1}$, $D_2 = D_3 = 2 \times 10^{-5} \text{ cm}^2 \text{ s}^{-1}$, $Z_1 = -4.5$. (Right axis) Dependence of osmotic modulus $c\partial\Pi/\partial c$ on J (\blacklozenge).

polymer concentration.¹ The semidilute solution can thus be pictured as an assembly of distinct charged particles, as in eq 1, with a hydrodynamic radius, a , and relaxation rate, Γ , described by eq 5. In this case, the diffusion coefficient is related to the structure factor, $S(q)$, by¹⁸

$$D(q, J) = D_0/S(q, J) \quad (11)$$

where D_0 is the value of $D(q, J)$ of the polymer segments, as in eq 6, at infinite dilution. The analog to eq 1 can therefore be written

$$I(q, J) = P(q) S(q, J) \quad (12)$$

where $P(q)$ is the form factor of the polymer chain segments.

Experimentally, as seen in Figure 9, the measured values of D_{NSE} are practically independent of J , having a mean value $3.0 \pm 0.2 \times 10^{-7} \text{ cm}^2 \text{ s}^{-1}$; that is, equal to D_{DLS} in the high ionic strength limit of the mode-coupling model. Furthermore, as noted in Figure 3, the scattered intensity, $I_{\text{coh}}(q)$, in the NSE region is also independent of J . The intensity is therefore governed only by the form factor $P(q) (\propto q^{-1})$ of the individual chain segments. It follows from eqs 11 and 12 that $S(q, J)$ is a constant, independent of both J and q , in accordance with the observed constancy of $D_{\text{NSE}}(q, J)$. This finding confirms the validity of eqs 11 and 12 at high q , where the scattering response is governed by local chain properties. It is pertinent to note that in semidilute HA solutions with zero added salt and in the absence of shear, no characteristic polyelectrolyte peak due to interchain correlation effects is observed in the structure factor $S(q, J)$.¹⁹

These findings are unexpected for two reasons: First, unlike semidilute solutions of neutral flexible polymers, the diffusion coefficient of the polymer segments, D_{NSE} , is the same as, and

not greater than the collective diffusion coefficient D_{DLS} at high J . Second, the NSE measurements show that decoupling is complete in the range $0.06 \leq q/\kappa \leq 1.6$, in apparent contradiction with the mode coupling model, which predicts decoupling only for $q/\kappa \gg 1$.

Conclusions

In semidilute solutions of the charged biopolymer HA in the physiological salt concentration range, the dynamic properties depend on the length scale of the measurement. At long length scales, coupling between the polymer and the ion cloud gives rise to a strong dependence on ionic strength, both of the collective diffusion coefficient and of the scattering structure factor. At short length scales both quantities are constant and independent of J . Decoupling from the ion cloud is observed in the range $0.06 \leq q/\kappa \leq 1.6$, which is smaller than the limit $q/\kappa \gg 1$ predicted by the mode coupling model.

Acknowledgment. We are grateful to the ILL, Grenoble, for access to the IN15, and to APS, Argonne, USA, for SAXS measurements. This research was supported by the Intramural Research Program of the NICHD, NIH.

References and Notes

(1) de Gennes, P. G. *Scaling Concepts in Polymer Physics*; Cornell: Ithaca, NY, 1979.

- (2) Muthukumar, M. *J. Chem. Phys.* **2004**, *120*, 9343.
 (3) Zhang, Y.; Douglas, J. F.; Ermi, B. D.; Amis, E. *J. Chem. Phys.* **2001**, *114*, 3299.
 (4) Mezei, F. *Neutron Spin Echo, Lecture Notes in Physics 128*; Springer: Berlin, 1980.
 (5) Hecht, A.-M.; Guillermo, A.; Horkay, F.; Mallam, S.; Legrand, J. F.; Geissler, E. *Macromolecules* **1992**, *25*, 3677.
 (6) Hecht, A.-M.; Horkay, F.; Schleger, P.; Geissler, E. *Macromolecules* **2002**, *35*, 8552.
 (7) Tivant, P.; Turq, P.; Drifford, M.; Magdelenat, H.; Menez, R. *Biopolymers* **1983**, *22*, 643.
 (8) Prabhua, V. M.; Amis, E. J.; Bossev, D. P.; Rosov, N. *J. Chem. Phys.* **2004**, *121*, 4424.
 (9) Berne, B. J.; Pecora, R. *Dynamic Light Scattering*; Wiley: New York, 1976.
 (10) Belloni, L.; Drifford, M.; Turq, P. *J. Phys. Lett. (Paris)* **1985**, *46*, 207.
 (11) Dobrynin, A. V.; Rubinstein, M. *Prog. Polym. Sci.* **2005**, *30*, 1049.
 (12) Geissler, E.; Hecht, A.-M.; Horkay, F. *Phys. Rev. Lett.* **2007**, *99*, 267801.
 (13) Horkay, F.; Basser, P. J.; Londono, D. J.; Hecht, A.-M.; Geissler, E. *J. Chem. Phys.* **2009**, *131*, 184902.
 (14) Cleland, R. L. *Arch. Biochem. Biophys.* **1977**, *180*, 57.
 (15) Hill, T. L. *Introduction to Statistical Thermodynamics*; Addison-Wesley: Reading, MA, 1960.
 (16) Schurr, J. M.; Bloomfield, V. *Crit. Rev. Biochem. Mol. Biol.* **1977**, *4*, 371.
 (17) Porod, G. In *Small Angle X-ray Scattering*; Glatter, O., Kratky, O., Eds.; Academic: London, 1982.
 (18) de Gennes, P. G. *Physica* **1959**, *25*, 825.
 (19) Villetti, M.; Borsali, R.; Diat, O.; Soldi, V.; Fukada, K. *Macromolecules* **2000**, *33*, 9418.

JP106578F